Synthesis and Characterizations of Calcium Di(meth)acrylate Divinyl Monomers and Melt Surface Graft Functionalization with Linear Low Density Poly(ethylene)

R. Anbarasan,[1,2] V. Dhanalakshmi,[2] K. Rajasulochana,[3] M. Sudha,[4] T. Jayalakshmi,[3] M. Anusuya[3]

[1]*Department of Chemical Engineering, Nano Biotechnology Research Laboratory, National Taiwan University, Taipei, Taiwan 10617, Republic of China*
[2]*Department of Polymer Technology, KCET, Virudhunagar, Tamil Nadu 626 001, India*
[3]*Department of Chemistry, SFR College for Women, Sivakasi, Tamil Nadu 626 123, India*
[4]*Department of Chemistry, N.S.College of Arts and Science, Theni, Tamil Nadu 625 531, India*

Received 2 February 2009; accepted 10 August 2009
DOI 10.1002/app.31257
Published online 15 October 2009 in Wiley InterScience (www.interscience.wiley.com).

ABSTRACT: Calcium diacrylate (CDA) and calcium dimethacrylate (CDM) divinyl monomers were synthesized by a solvo thermal method. The FTIR spectra showed a peak at 1650 cm^{-1} due to the presence of a C=C for both CDA and CDM. Proton NMR and carbon NMR confirmed the structure of CDA and CDM synthesized by a solvo thermal method. DSC determined the melting temperatures of CDA and CDM. XRD indicated the presence of a d_{110} plane peak for CDA and CDM. The % weight residue that remained above 700°C in TGA method confirmed the higher thermal stability of CDA. Thus, synthesized CDA and CDM were surface grafted on linear low density poly(ethylene) (LLDPE) at 160°C under inert atmosphere by thermolysis method. FTIR confirmed the presence of C=O stretching due to CDA and CDM in LLDPE backbone after thermolysis reaction. ^{1}H-NMR confirmed the chemical grafting of CDM onto LLDPE. © 2009 Wiley Periodicals, Inc. J Appl Polym Sci 115: 2582–2590, 2010

Key words: melt functionalization; FTIR; DSC; TGA; NMR; XRD; kinetics

INTRODUCTION

Recently, the applications of polyolefins are restricted to some extent because of the absence of polar or hydrolysable group on the polyolefin backbone and causes environmental pollution. To solve this problem, polyolefins are functionalized with different functional groups. Among those, metal acrylates and metal methacrylates play a vital role in the functionalization (process) of polyolefins. During the bio-degradation process, the polymer backbone undergoes degradation at four points due to the grafted metal acrylates or metal methacrylates. Keeping this point in mind, we started the synthesis of such metal acrylates as the first step. Vela et al.[1] reported solid state polymerization of bis(but-3-enolate) zinc. Gamma ray irradiated solid state polymerization of bis(but-3-enolato) calcium resulted with very high molecular weight was also reported in the literature.[2] FTIR spectroscopy method was used to follow the course of *in situ* polymerization of zinc dimethacrylate in poly(oxyethylene) elastomer.[3] Various research teams[4–9] carried out the solid state polymerization of calcium dimethacrylate (CDM) and barium methacrylate. Iketa[10,11] reported free radical copolymerization of zinc dimethacrylate with hydroxylated nitrile butadiene rubber. Effect of zinc dimethacrylate and CDM monomers on the bond strength of polymers were reported in the literature.[12] Copolymerization of zinc dimethacrylate and perfluoroalkyl acrylate in benzene was reported in the literature.[13] The structure and magnetic properties of Fe (II) and Co (II) acrylate complexes were investigated by Lawecker et al.[14] The kinetic peculiarities of the thermal transformation of unsaturated metal carboxylates and properties of metal polymer nano composites formed have been studied.[15] By thorough literature survey we could not find any report based on the functionalization of linear low density polyethylene (LLDPE) with metal acrylates and metal methacrylates. In the present investigation, we took this job as a challenge and successfully synthesized the calcium diacrylate (CDA) and CDM divinyl monomers and functionalized the LLDPE backbone with CDA and CDM.

Correspondence to: R. Anbarasan (anbu_may3@yahoo.co.in).

Contract grant sponsor: DST; contract grant number: SR/FTP/CS-39/2005.

FTIR spectrometer is a useful tool in various science and engineering fields, because of its high sensitivity or detectivity towards the trace amount of sample and low noise to signal ratio. Moreover, this method is easy and inexpensive one. FTIR spectroscopy is used in both qualitative[16–21] and quantitative[22–32] applications. The above literature survey indicates that FTIR kinetic reports on functionalization of LLDPE with metal salts are not available. In the present investigation, we have reported the synthesis, characterizations and surface melt grafting of CDA and CDM with LLDPE backbone by thermolysis method. Surface grafting of CDA or CDM onto LLDPE backbone was quantitatively followed by the FTIR based simple kinetic method for the first time.

EXPERIMENTAL

Materials

Calcium carbonate (SD Fine Chemicals, AR grade, India), acrylic acid (Merck, India), and methacrylic acid (SD Fine Chemicals) were purchased and used as received. LLDPE (Rayson, India, M_w-1,25,000 Da) was purchased and purified by the procedure followed in our earlier publication.[30] Toluene (Chemspure, AR, India) and acetone (Merck) were received and used without further purification. Dicumyl peroxide initiator (DCP, Across Chemicals, UK) and cyclohexane (Paxy chemicals, AR, India) were used as received.

Synthesis of calcium diacrylate and calcium dimethacrylate

Ten gram of $CaCO_3$ was dissolved in 200 mL of doubly distilled water in a three-necked round bottom (RB) flask; 10 mL of methacrylic acid was added drop by drop to the $CaCO_3$ solution followed by 0.03 g of antimony trioxide, the esterification catalyst, to catalyze the metal ester formation process. The contents were sparged with nitrogen gas to create an inert atmosphere inside the flask. The RB flask was connected to a water condenser and the solution was boiled for 3 h continuously, with vigorous stirring at 90°C. Finally, the precipitate was washed with acetone and the sample was dried, weighed and stored in a zipper bag.

Purification of LLDPE

Five gram of LLDPE pellet sample was dissolved in 100 mL of toluene solvent at 130°C for 3 h to remove antioxidants added during its long storage process. Once all the LLDPE powder samples were dissolved in toluene, then cool it and 800 mL of acetone was added to precipitate the LLDPE.[30] The contents were filtered and dried at 60°C for 24 h under vacuum. The dissolution and precipitation process were repeated three times to further purify the LLDPE. Finally, the dried samples were weighed and stored in a zipper bag.

Synthesis of LLDPE-*g*-CDM

One gram of pure LLDPE powder sample was added with 5% weight of CDA or CDM in 25 mL of cyclohexane-dichloromethane (1 : 9 v/v) solvent mixture in a 100 mL beaker with mild stirring. The solvent mixtures were used to distribute the DCP and CDM or CDA onto LLDPE backbone uniformly, otherwise agglomeration occurred. Then, 5% weight of DCP was mixed with the content of the beaker and the stirring was continued for 1 h. In the present investigation, both DCP and metal acrylate and metal methacrylate were used in equal concentrations, particularly, with 1 : 1 ratio, after many trial experiments. After 1 h of mixing, the solvent was removed by rotary evaporation. Transfer the reaction mixture into a test tube reactor and de-aerate the same for 30 min with sulfur free nitrogen gas. After degassing, the reactor was kept in an oil bath at 160°C for 2.5 h without stirring. After functionalization was completed, the reactor was removed from the oil bath, cooled to room temperature, and the functionalized LLDPE samples were collected and cut into small pieces. These were put in toluene at 130°C for 30 min for the isolation purpose. The functionalized, non-crosslinked samples dissolved in toluene while the functionalized crosslinked samples did not dissolve in toluene. The dissolved samples were re-precipitated by adding 600 mL of acetone and the crosslinked samples were isolated. The non-crosslinked sample was collected and dried under vacuum at 60°C. After drying, the sample was weighed and stored in a zipper bag. FTIR spectrum was obtained and quantitative calculations have done with the non-crosslinked, functionalized polymers. For proton NMR study, the non-crosslinked and functionalized polymer sample was dissolved in dueterated toluene and NMR spectrum was recorded at 80°C.

Characterizations

FTIR spectra were recorded using 8400 S Shimadzu FTIR spectrometer by KBr pelletization method from 400 to 4000 cm^{-1}. Proton and carbon NMR spectra were recorded using Bruker instrument in D_2O (for CDM and CDA) and toluene-D medium (for CDM or CDA surface grafted LLDPE sample). TGA was recorded using Universal V4.3A TA instrument under air atmosphere from room temperature to 800°C at the heating rate of 10°C/min. DSC of the

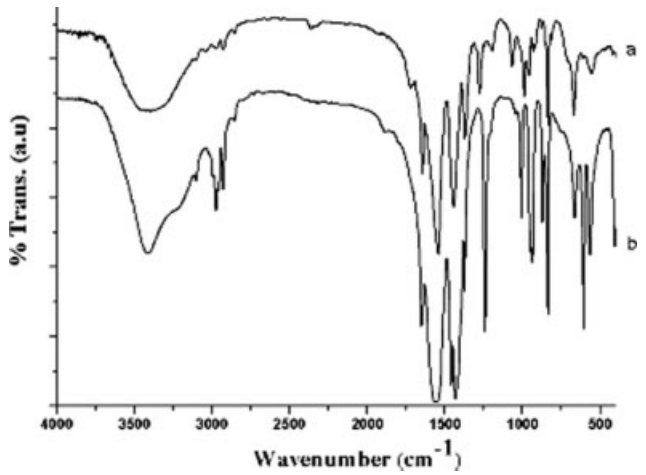

Figure 1 FTIR spectrum of CDA and CDM.

sample was recorded using Universal V4.3A TA instrument under nitrogen atmosphere at the heating rate of 10°C/min from room temperature to 120°C. XRD was recorded using Rigaku Rint 2000 (Japan) diffractometer at room temperature with CuKα1 radiation from the 2Θ value of 2 to 70°. The angle 2Θ was scanned from 2 to 60°. The voltage and current of X-ray tubes were 40 kV and 100 mA, respectively. Elemental analysis was carried out using Elementor GmbH Vario El instrument.

RESULTS AND DISCUSSION

For the sake of convenience, the results and discussion part is sub-divided into two parts namely: (i) characterizations of CDA and CDM divinyl monomers and (ii) characterizations of CDM and CDA functionalized LLDPE. Let us discuss one by one.

Characterizations of CDA and CDM divinyl monomers

FTIR study

Figure 1(a,b) represent the FTIR spectra of CDA and CDM, respectively. The FTIR spectrum confirmed the functional groups present in CDA and CDM. The metal oxide stretching was appeared at 540 cm^{-1}, the C—H out of plane bending vibration could be seen at 829 cm^{-1} and the metal ester stretching was signed at 978 cm^{-1}. Peaks between 1400 and 1500 cm^{-1} represented the carbonyl symmetric and anti-symmetric stretching vibrations. The C=C in CDM or CDA was confirmed by a peak at 1640 cm^{-1}. A small hump at 1714 cm^{-1} confirmed the presence of carbonyl stretching. Generally, the carbonyl stretching is very sharp, but in the present study, due to the influence of calcium ions on the ester carbonyl group, the intensity of carbonyl peak is depressed drastically. Peaks around 2800–3000 cm^{-1} informed the C—H symmetric and anti-symmetric stretching vibrations of acrylate group. A broad peak from 3000 to 3500 cm^{-1} was due to the OH stretching of water molecules associated with the metal diacrylates and dimethacrylates.

NMR spectra

Figure 2 shows the proton NMR spectrum of CDM with five peaks. Proton NMR was recorded in D_2O solvent and hence a peak due to the presence of water was appeared at 4.7 ppm. The methyl proton in CDM can be seen at 1.69 ppm with a peak integration value of 2.66. This argued the presence of two methyl groups in CDM. Another one peak that signed at 5.18 ppm was associated with the methylene protons (CH_2). Apart from these, two new peaks corresponding to CDA was also appeared. CDA was formed as a by-product during the synthesis, through atom transfer reactions. A signal at 5.50 ppm is corresponding to the methylene group of CDA. The methine proton of CDA is appeared between 5.80 and 6.00 ppm. The proton NMR confirmed that some amount of CDA was also formed as a by-product by atom transfer reaction, during the preparation of CDM. Figure 3 represents the ^{13}C-NMR spectrum of CDM. Seven peaks are appeared in ^{13}C-NMR spectrum. The first peak that appeared at 18.7 ppm was due to the methyl carbon of CDM. Another peak at 120 ppm was due to the methylene carbon of CDA. The methylene carbon of CDM is

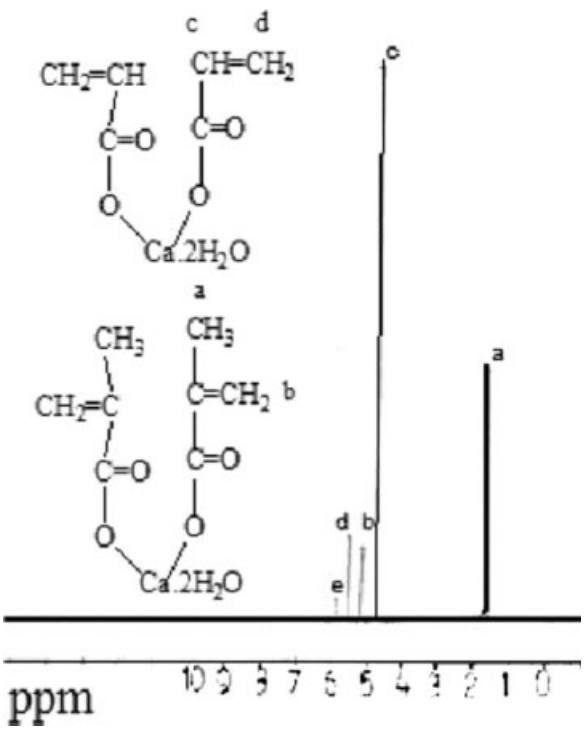

Figure 2 ^{1}H-NMR spectrum of CDM.

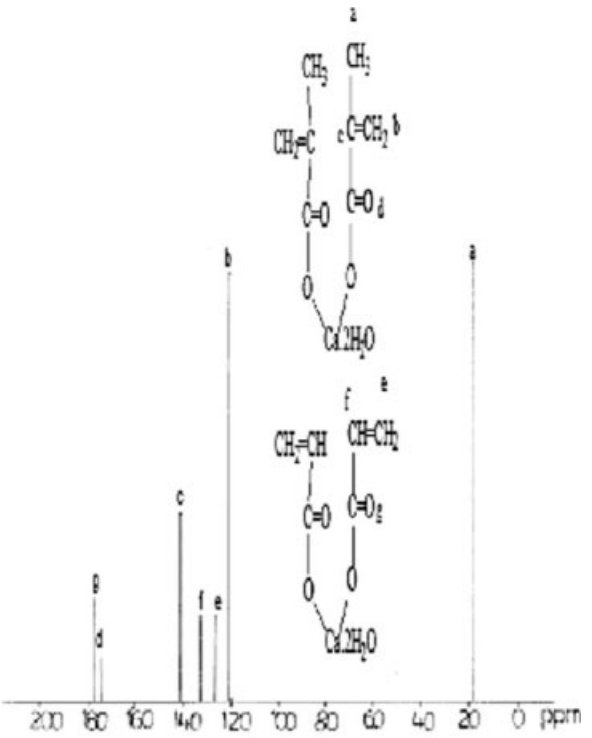

Figure 3 ^{13}C-NMR spectrum of CDM.

appeared at 120.69 ppm. The methine carbon of CDA has appeared at 133.41 ppm. A signal at 141.94 ppm is due to the tertiary carbon atom of CDM. In the ^{13}C-NMR spectrum, two new peaks are remaining due to the carbonyl carbon atom of CDM and CDA. The carbonyl carbon atom of CDM is appeared at 175.65 ppm whereas the carbonyl carbon atom of CDA is appeared at 177.65 ppm. Appearance of these peaks confirmed the presence of CDA in CDM monomer.

TGA

Figure 4 represents the TGA thermogram of CDA and CDM. Here, the TGA and FTIR spectrometer instruments were not coupled during the TGA measurement. TGA of CDA is shown in Figure 4(a). The thermogram showed a three-step degradation process. The first minor weight loss step up to 250°C was due to the removal of physisorbed and chemisorbed water molecules. The second major weight loss step was due to the dissociation of CDA bond

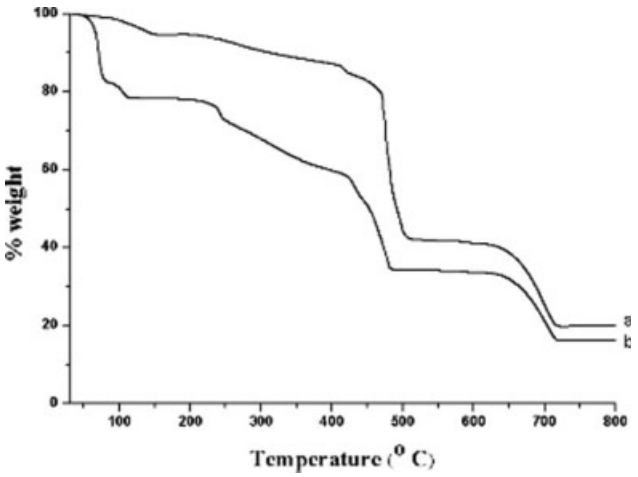

Figure 4 TGA of (a) CDA and (b) CDM.

and the dissociation extended up to 510°C. The third minor weight loss step was ascribed to the removal of CO_2 from acrylates. Here, the second and third degradation steps are very important because they give an idea about the degradation temperature of CDA monomer. During the degradation process, first the metal ester sigma bond had broken down followed by the liberation of CO_2 from the ester linkage. On further heating, the metal ion reacted with the surrounding air and resulted with the formation of a stable metal oxide. That explained the thermal stability of divinyl monomer like CDA. Figure 4(b) represented the TGA of CDM. The thermogram showed a four-step degradation process. The first minor weight loss below 100°C was associated with the removal of moisture and physisorbed water molecules. The second minor weight loss step extended up to 400°C can be explained on the basis of removal of water molecules, chemically binding with the central metal ion. The major weight loss extended up to 485°C was due to the dissociation of metal acrylate bond. The last minor weight loss step was due to the removal of CO_2 from acrylate group. In the present investigation, the second, third, and fourth degradation steps are very important because they explained the thermal stability of the divinyl monomer. The data is mentioned in Table I. On overall comparison, CDA showed higher thermal stability than CDM. The % weight residue remained above 700°C confirmed the char forming capability of CDA as well as CDM. Between the two, CDA

TABLE I
TGA Data of CDA and CDM

System	% Weight at 200°C	% Weight at 400°C	% Weight at 500°C	% Weight at 600°C	% Weight above 600°C
CDA	94.2	87.1	45.6	41.2	20.1
CDM	78.4	59.7	34.2	33.3	16.1

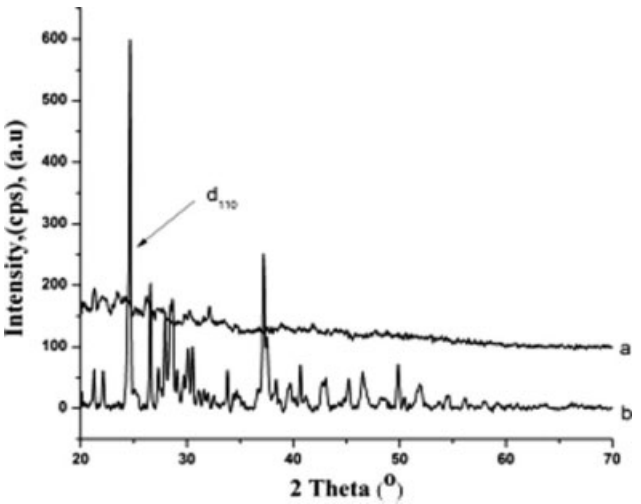

Figure 5 XRD of (a) CDA and (b) CDM.

showed higher char forming capability. The molar mass (GPC), surface morphology (SEM), and reinforcement High Resolution Transmission Electron Microscopy (HRTEM) are now under investigation in our lab.

XRD

Figure 5 indicates the XRD of CDA and CDM. The d_{110} plane corresponding to the layered structure of calcium ions [Fig. 5(a)—CDA] appeared at the 2Θ value of 24.7° but with lower intensity. The other crystal planes are also appeared. Peaks with lower intensity described the semi crystalline nature of CDA. Figure 5(b) indicated the XRD of CDM. Here, also the aforementioned crystalline peaks are seen but with higher intensity. This indicated that the central calcium ion and acrylate carbon atoms were arranged in the respective lattice points exactly. This inferred that the presence of methyl substituent restricted the carbon–carbon rotation in CDM.

DSC

Figure 6(a) represents the DSC of CDA. The thermogram showed three endothermic peaks with the melting temperature at 85°C. The endothermic peaks that appeared below 70°C are associated with the internal rearrangement of microstructures. Figure 6(b) shows only one endothermic peak at 91.7°C due to the melting of CDM. The internal conversion of microstructure did not appear in CDM.

Elemental analysis

Further, the structural composition of CDA and CDM was confirmed by elemental analysis. CDA gave the following details: C-35.48%, H-5.62%, O-58.89% that accounted for the following structural formula $C_6H_6O_4Ca{\cdot}2H_2O$. CDM produced the following data on elemental analysis. C-37.08%, H-3.51%, O-59.40% which supported for the following structural formula $C_8H_{10}O_4Ca{\cdot}2H_2O$.

The LLDPE was functionalized with CDA and CDM by thermolysis method. Aim of this functionalization method was to introduce an ester functional group onto LLDPE backbone at the same time during the bio-degradation process the degradation proceeded at four points and led to the pollution free environment. During the bio-degradation of LLDPE-*g*-CDM/CDA, liberation of CO_2 with rapid macro chain degradation will take place.

Characterizations of CDM and CDA functionalized LLDPE

FTIR study on LLDPE-*g*-CDA and CDM

It is well known that during the melt functionalization of polyolefins, carbon–carbon double bond with simultaneous functionalization will be formed due to thermal oxidation reactions. Our aim is to find out the amount of double bond formed with simultaneous grafting of CDM and CDA onto LLDPE backbone. In the present investigation, we intend to present a report about the reaction for the CDM or CDA surface grafted LLDPE based on FTIR results for the first time.

Figure 7 represents the FTIR spectra of LLDPE after functionalization with CDA at different percentage weights ratio. The important peaks are characterized below: 717 cm^{-1} —CH out of plane bending vibration, 1077 cm^{-1} —C—O—Ca linkages, 1563 cm^{-1} —C=C, 1715 cm^{-1} —C=O stretching. C—H symmetric stretching vibration appeared at 2625 cm^{-1} and C—H anti-symmetric stretching vibration appeared as a broad peak at 2883 cm^{-1}. Apart from these, another broad peak appeared at higher wave

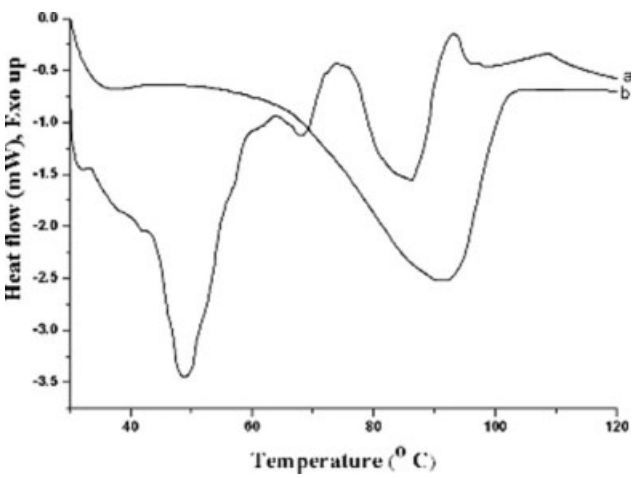

Figure 6 DSC of (a) CDA and (b) CDM.

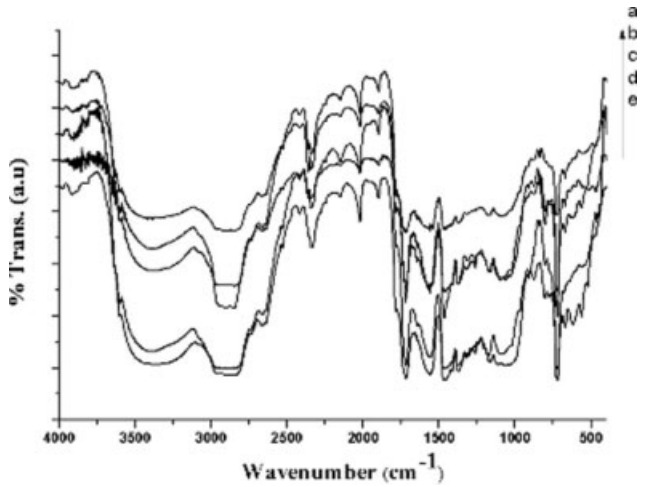

Figure 7 FTIR spectrum of LLDPE grafted with CDA at (a) 1% weight, (b) 3% weight, (c) 5% weight, (d) 7% weight, and (e) 9% weight.

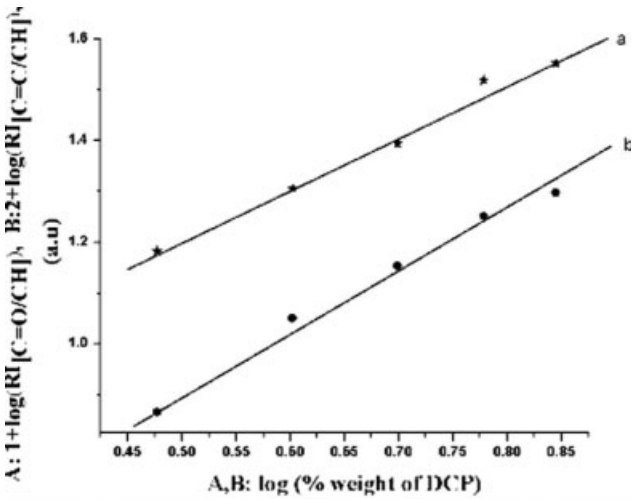

Figure 8 Effect of (% weight of DCP) on RI of (a) carbonyl and (b) alkene in LLDPE-*g*-CDA system.

number (3000–3500 cm^{-1}) due to the OH stretching vibration of water molecule attached to the metal esters.

During the melt surface graft functionalization process, DCP and metal ester concentrations were used equally. The % weight of DCP was varied between 1 and 9. After thermolysis reaction, the relative intensity of $RI_{[A1715/A717]}$ increased with the increase of % weight of DCP. It meant that if we increase the % weight of DCP or CDA, the % grafting of metal ester onto LLDPE backbone would also increase. Figure 7 shows the FTIR spectra of LLDPE functionalized with CDA at different % weight. We found two interesting facts. By increasing the % weight of CDA during melt functionalization process, the RI of C=O as well as RI of C=C was increasing simultaneously in a considerable quantity. Hence, we were in a position to find out the order of reaction for the metal ester functionalization as well as olefin bond formation. To find out the order of reaction for metal ester functionalization reaction, the log (% weight of DCP) versus log ($RI_{[C=O/CH]}$) was plotted [Fig. 8(a)]. The plot showed a straight line with a slope value of 1.01, which confirmed the first order melt surface graft functionalization reaction with respect to (% weight of DCP) or (% weight of CDA). This indirectly led to the unimolecular termination reaction. The other interesting aspect was in finding the order of olefin bond formation during the thermolysis reaction. Again, the log–log plot was made between (% weight of DCP) and log ($RI_{[C=C/CH]}$) [Fig. 8(b)]. The plot showed a straight line with a slope of 1.11. This indicated the first order reaction of double bond formation with respect to (% weight of DCP) or (% weight of CDA). The C=C bond formation during the surface melt graft functionalization reaction was explained as follows: The first and foremost reason is thermal oxidation reaction, second, due to the intermolecular H_2 transfer reaction and finally the double bond may be formed at the middle of the LLDPE chain or it may be formed at the end of the LLDPE chain.

Figure 9 represents the FTIR spectrum of LLDPE after melt functionalization with different (% weight of CDM). Here also one can observe the same FTIR characteristic peaks as mentioned earlier, which confirmed the surface melt grafting of CDM onto LLDPE backbone. Also, the $RI_{[C=O/CH]}$ as well as $RI_{[C=C/CH]}$ increased with the increase of (% weight of DCP). The order of reaction for surface melt functionalization [Fig. 10(a)] and olefin formation [Fig. 10(b)] was determined as 1.0 and 1.0, respectively, which again confirmed the first order reaction for both functionalization and C=C formation similar to LLDPE–CDA system.

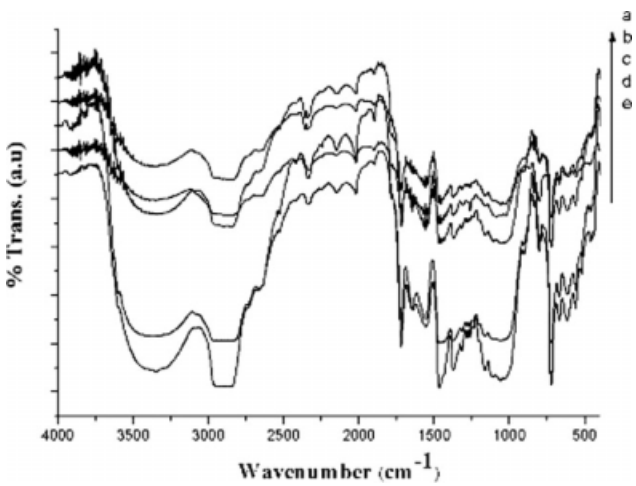

Figure 9 FTIR spectrum of LLDPE grafted with CDM at (a) 1% weight, (b) 3% weight, (c) 5% weight, (d) 7% weight, and (e) 9% weight.

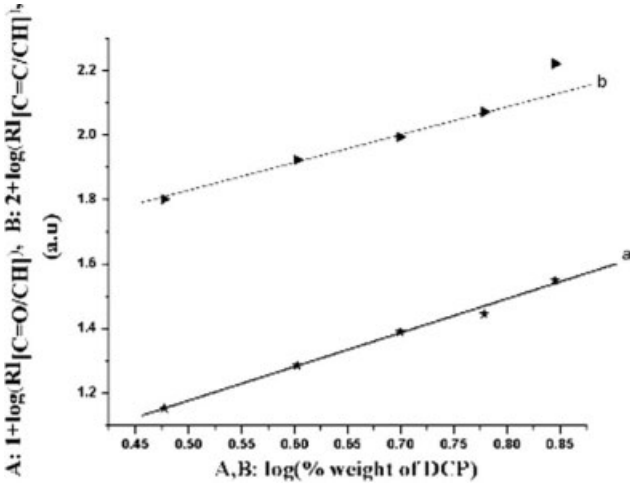

Figure 10 Effect of (% weight of DCP) on RI of (a) [C=O/CH] and (b) [C=C/CH] in LLDPE-*g*-CDM system.

For the sake of comparison, the FTIR spectrum of pristine LLDPE is represented in Figure 11. The important peaks are explained below. A twin broad peak at 2654 and 2901 cm^{-1} are due to the C—H symmetric and anti-symmetric stretching. CH_2 stretching is exhibited at 1475 cm^{-1}. The C—H out of plane bending vibration is appeared at 726 cm^{-1}. Absence of a peak around 1730 cm^{-1} declared the absence of carbonyl group on the LLDPE backbone. Hence, a peak corresponding to carbonyl group is only due to the grafted CDA or CDM in Figures 8 and 10, respectively. The grafted carbonyl group after functionalization process is associated with the free radical grafting of CDA or CDM or acetophenone onto LLDPE backbone. Chemical grafting of acetophenone onto LLDPE backbone is less feasible route due to higher reaction temperature. This informed us that the carbonyl group is surely due to the grafted CDA or CDM onto the LLDPE backbone.

^{1}H-NMR analysis of LLDPE-*g*-CDM

Figure 12 represents the proton NMR spectrum of CDM grafted LLDPE. The spectrum showed the peak corresponding to CDM. However, our aim is to prove the chemical grafting of CDM onto LLDPE backbone, so that the peaks due to LLDPE should be explored. In the proton NMR spectrum particularly, we have concentrated on the chemical shift value of 5 to 6 ppm because only in this range we have new peaks corresponding to LLDPE (in functionalized and oxidized form). Because of the thermal and peroxide treatment, LLDPE underwent various chemical reactions such as chain degradation, chain scission, alkenes formation (the double bond may be formed at the end of LLDPE chain or at the middle of LLDPE chain), unsaturated aldehyde formation, etc. In the present investigation, the appearance of new

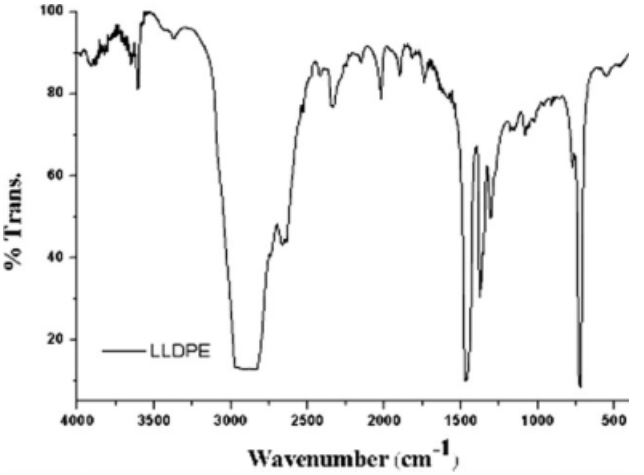

Figure 11 FTIR spectrum of pristine LLDPE.

peaks is due to the alkenes formation, during the functionalization process. Appearance of a broad peak at 1.91 ppm confirmed the methylene proton of LLDPE (Figure not shown here). Appearance of these new peaks confirmed the chemical grafting of CDM onto LLDPE backbone.

Mechanism

Anbarasan et al.[30] explained the mechanism of free radical grafting of thioester onto HDPE backbone. Similar type of mechanism is applied here. However, the presence of two double bonds at the ends leads to different possible reactions. Seetharaman and Gopalan[33] explained the polymerization of

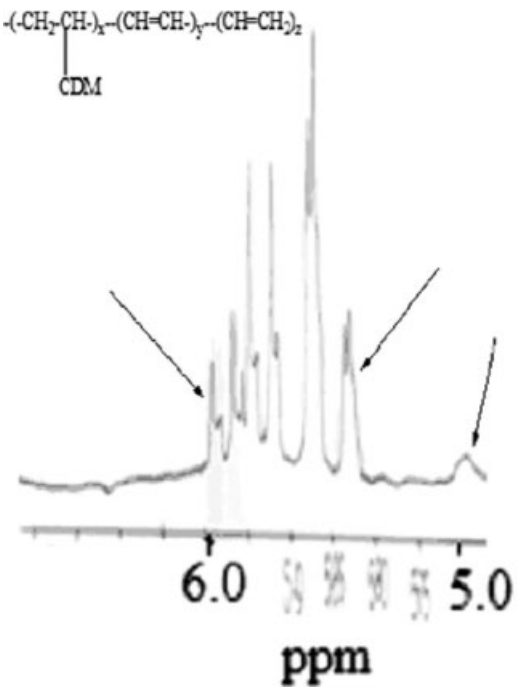

Figure 12 ^{1}H-NMR spectrum of LLDPE-*g*-CDM.

divinyl monomers via cyclization mechanism because of 1,7 interactions and they reported cyclic product formation during the ultrasound initiated polymerization of aqueous solutions of diallyl dimethyl ammonium chloride. Similar type of mechanism is applied here. During the melt functionalization process, grafting of cyclic polymer is also a possible route. Melt functionalization reaction proceeds via free radical reaction. Free radical reactions precede through three steps namely initiation, propagation and termination reactions. The mechanism is represented below:

DCP, the free radical initiator, produced two cumyloxy radicals on heating to 160°C at the normal dissociation rate. Formations of free radicals are the initiation step of melt functionalization reaction. On comparing the initiation efficiency of cumyloxy radicals and methyl radicals, the later one is more aggressive in nature at a given temperature. Thus, formed free radicals interacted with LLDPE and CDA or CDM led to the various processes. In the present investigation, we had used 1 : 1 : 1 ratio of LLDPE, CDM or CDA and DCP. Because 1 mol of DCP is required to initiate 1 mol of LLDPE and 1 mol of CDA or CDM. Hence, we used the equal concentrations of DCP and CDA or CDM. The experimental results indicated that both the ester functionalization and alkene formation processes followed the first order reaction with respect to % weight of DCP. During the ester functionalization reaction, simultaneous graft copolymerization of CDM or CDA onto LLDPE backbone is also favorable one. In such a way the RI of [C=O/CH] increased with the increase of % weight of DCP. In the case of alkene formation, here also the RI of [C=C/CH] increased with the simultaneous increment with DCP. Alkene formation occurred with two possibilities due to thermal degradation reactions. The first one associated with the terminal double bond whereas the second one dealt with the middle double bond. Among these two, the most probable route is the terminal double bond formation. Because the LLDPE chain end with coil like structure exposed its tail to the reaction medium and experienced the chemical reactions. Meanwhile, coupling of LLDPE macro radicals led to the cross linking reactions. By this way, the experimental results obtained through various chemical reactions and proposed reactions schemes are matching with each other.

Initiation

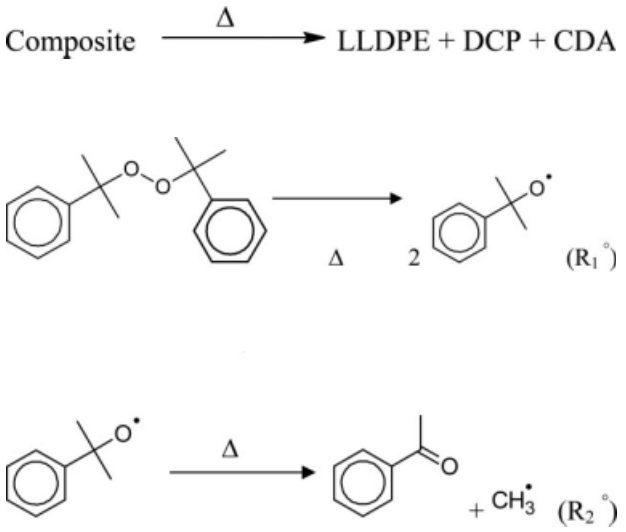

Propagation

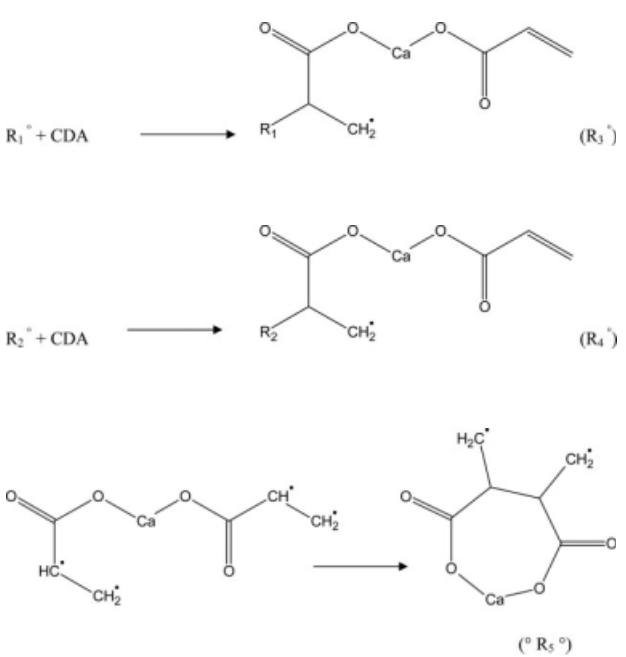

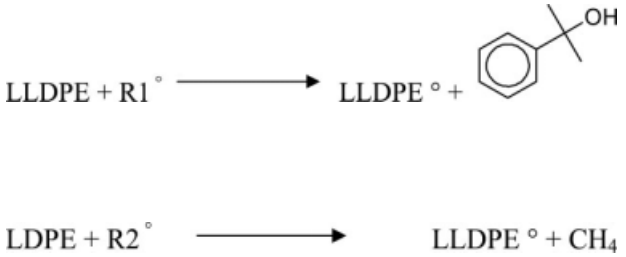

Termination

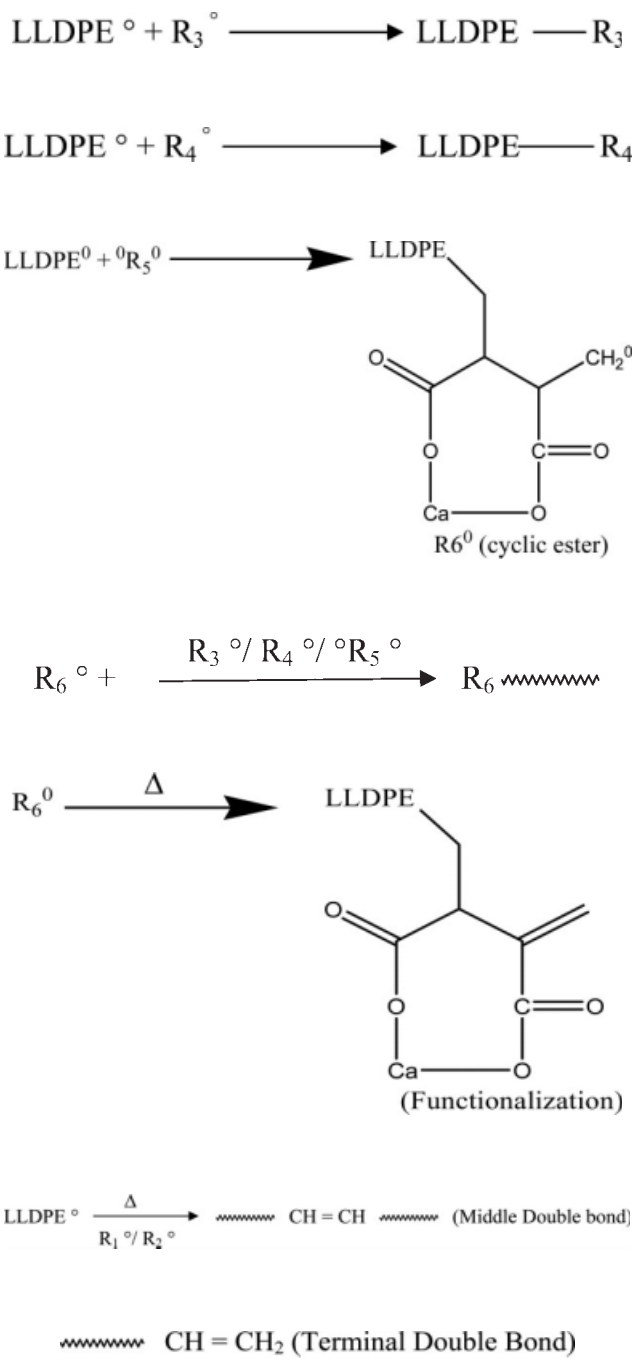

CONCLUSIONS

Calcium diacrylate and dimethacrylate divinyl monomers were successfully synthesized by a solvo thermal method and were confirmed by FTIR (1650 cm^{-1}) and proton NMR (5.18 ppm) spectra. XRD confirmed the presence of a d_{110} crystal plane of central calcium ion. The melting temperature of CDA and CDM were determined as 85°C°C and 91.7°C, respectively. The higher char forming (20%) behavior of CDA was confirmed by TGA method. The FTIR relative intensity measurements confirmed the first order reaction for both metal ester functionalization and olefin bond formation for CDA and CDM. ^{1}H-NMR confirmed the chemical grafting of CDM onto LLDPE backbone by showing new peaks between 5 and 6 ppm.

References

1. Vela, M. J.; Buchholz, V.; Foxman, B. M. Chem Commun 2000, 2225.
2. Vela, M. J.; Snider, B. B.; Foxman, B. M. Chem Mater 1998, 10, 3167.
3. Lu, Y.; Lu, L.; Shen, D.; Yang, C.; Zharg, L. Polym Int 2004, 53, 802.
4. Lando, J. S.; Morawetz, H. J Polym Sci Chem Ed 1964, 4, 789.
5. Coastaschuk, F. M.; Crisson, D. F. R. Macromolecules 1970, 3, 393.
6. Coastaschuk, F. M.; Crisson, D. F. R. J Phys Chem 1970, 74, 2035.
7. Coastaschuk, F. M.; Crisson, D. F. R. Macromolecules 1971, 4, 16.
8. Donnell, J. H. O.; Mecarvey, B.; Morawetz, H. J Am Chem Soc 1964, 86, 2324.
9. Lepage, Y.; Forteir, S.; Donnay, G. J Polym Sci Chem Ed 1978, 16, 2265.
10. Iketa, J.; Yamoda, B. Polym Int 1999, 48, 367.
11. Ahn, N. J Appl Polym Sci 2003, 90, 991.
12. Iketa, J.; Sakurai, S.; Yamoda, B. J Appl Polym Sci 1996, 59, 781.
13. Iketa, J.; Yamoda, B.; Tsaji, M.; Sakurai, S. Polym Int 1999, 48, 446.
14. Lawlecka, M.; Kopcewicz, M.; Pomogailo, A. D. J Nanopart Res 2003, 4, 373.
15. Pomogailo, A. D.; Muraviev, D. N. J Nanopart Res 2003, 5, 497.
16. Hameed, S. F.; Allam, M. A. J Appl Sci Res 2006, 2, 27.
17. Chakraborty, S.; Bandyopadhyay, S.; Dueri, A. S. Polym Test 2007, 26, 38.
18. Svegl, F.; Orel, B. Mater Technol 2003, 37, 29.
19. Copikova, J.; Synytsya, A.; Novethna, M. Czech J Food Sci 2001, 19, 51.
20. Wang, J. S.; Shi, J. S.; Wu, J. G. World J Gastroenterol 2003, 9, 1897.
21. Xueref, I.; Domine, F. Atmos Chem Phys 2003, 3, 1779.
22. Matkovic, S. M.; Valle, G. M.; Briand, L. E. Lat Am Appl Res 2005, 35, 189.
23. Schwendner, K.; Libowitsky, E.; Koss, S. Geophys Res Abstr 2003, 5, 06826.
24. Asimow, P. D.; Stein, L. C.; Rissman, G. R. Am Mineral 2006, 91, 278.
25. Van De Voort, F. R.; Sedman, J.; Mucciardi, C. Appl Spectrosc 2004, 58, 193.
26. Parker, J. R.; Waddell, W. H. J Elast Plast 1996, 28, 140.
27. Saule, M.; Navarre, S.; Babot, O.; Maillard, B. Macromolecules 2003, 36, 7469.
28. Saule, M.; Navarre, S.; Babot, O.; Maillard, B. Macromolecules 2005, 38, 77.
29. Navarre, S.; Maillard, B. J Polym Sci Part A: Polym Chem 2000, 38, 2957.
30. Anbarasan, R.; Babot, O.; Dequiel, M.; Maillard, B. J Appl Polym Sci 2005, 97, 761.
31. Anbarasan, R.; Babot, O.; Dequiel, M.; Maillard, B. J Appl Polym Sci 2005, 97, 766.
32. Duraimurugan, K.; Rathiga, S.; Anbarasan, R. Chin J Polym Sci 2008, 26, 393.
33. Seetharaman, V.; Gopalan, A. Ind J Pure Appl Phys 2004, 42, 735.